ELSEVIER

Earth and Planetary Science Letters 195 (2002) 141–153

EPSL

www.elsevier.com/locate/epsl

Isotopic fractionation between Fe(III) and Fe(II) in aqueous solutions

Clark M. Johnson [a,*], Joseph L. Skulan [a], Brian L. Beard [a], Henry Sun [b], Kenneth H. Nealson [b], Paul S. Braterman [c]

[a] *Department of Geology and Geophysics, University of Wisconsin, Madison, WI 53706, USA*
[b] *Jet Propulsion Laboratory, 4800 Oak Grove Dr., Pasadena, CA 91109, USA*
[c] *Department of Chemistry, University of North Texas, Denton, TX 76203, USA*

Received 31 January 2001; accepted 1 November 2001

Abstract

Large equilibrium isotope fractionation occurs between Fe(III) and Fe(II) in very dilute (≤22 mM Cl^-) aqueous solutions, reflecting significant differences in bonding environments. Separation of Fe(III) and Fe(II) is attained by rapid and complete precipitation of Fe(III) through carbonate addition, followed by separation of supernatant and ferric precipitate; experiments reported here produce an equilibrium $\Delta_{Fe(III)-Fe(II)} = +2.75 \pm 0.15$‰ for $^{56}Fe/^{54}Fe$ at room temperature (22 ± 2°C). The timescales required for attainment of isotopic equilibrium have been determined by parallel isotope tracer experiments using ^{57}Fe-enriched iron, which are best fitted by a second-order rate law, with $K = 0.18 \pm 0.03$ s^{-1}. Based on this rate constant, ~15–20% isotopic exchange is estimated to have occurred during Fe(III)–Fe(II) separation, which contributes < 0.10‰ uncertainty to the equilibrium $\Delta_{Fe(III)-Fe(II)}$. Under the experimental conditions used in this study, >97% Fe(II) exists as $[Fe^{II}(H_2O)_6]^{2+}$, and >82% Fe(III) exists as $[Fe^{III}(H_2O)_6]^{3+}$ and $[Fe^{III}(H_2O)_{6-n}(OH)_n]^{3-n}$; assuming these are the dominant species, the measured Fe isotope fractionation is approximately half that predicted by Schauble et al. [Geochim. Cosmochim. Acta 65 (2001) 2487–2497] at 20–25°C. Although this discrepancy may be due in part to the experimentally unknown isotopic effects of chloride interacting with Fe-hexaquo or Fe-hydroxide complexes, or directly bonded to Fe, there still appears to be at this stage a >1‰ difference between prediction and experiment.

Keywords: ferric iron; ferrous iron; stable isotopes; oxidation; reduction; fractionation

1. Introduction

Iron isotope geochemistry recently has become quite prominent, because of its potential for tracing the geochemical cycling of Fe. The biologically produced Fe isotope fractionation that occurs during bacterial Fe reduction suggests that Fe isotope geochemistry may be applied to outstanding problems such as the origin and evolution of life on Earth or other planetary bodies [2,3]. Although it is clear that Fe isotopes are fractionated in biological processes, and thus may be a potential 'biosignature', the extent of

* Corresponding author. Tel.: +1-608-262-1710; Fax: +1-608-262-0693.
E-mail address: clarkj@geology.wisc.edu (C.M. Johnson).

0012-821X/02/$ – see front matter
PII: S0012-821X(01)00581-7

abiologic or inorganic Fe isotope fractionation remains largely unknown. Abiologic isotopic fractionations on ion exchange columns have been noted by Anbar et al. [4], although the applicability of these experiments, which involved highly acidic, high-ionic-strength solutions, to natural systems is unclear. Kinetic isotope fractionation between Fe(III) and Fe(II) complexes has been inferred in complex experiments that additionally record fractionation during ion exchange separation and species dissociation [5]. In addition, Fe isotope fractionation between aqueous species has been inferred from precipitation experiments in steady-state, flow-through reactors [6]. It is important to note, however, that in none of these cases [4–6] could isotopic equilibrium be clearly established. Because large ranges in Fe isotope compositions in nature are only found in rocks and minerals that formed at low temperatures [2,3,7], it is important to determine to what extent such ranges could have arisen by abiological fractionation through experiments that demonstrate attainment of isotopic equilibrium.

Several workers have predicted significant equilibrium Fe isotope fractionations based on spectroscopic data. Modeling ^{57}Fe Mössbauer data, Polyakov and Mineev [8] predict Fe isotope fractionations on the order of several per mil at moderate temperatures, where, for example at 125°C, a 3–4‰ *equilibrium* isotope fractionation in ^{56}Fe/^{54}Fe is calculated between siderite and pyrite, or siderite and magnetite. Schauble et al. [1] have predicted Fe isotope fractionations for coexisting aqueous Fe species, combining a modified Urey–Bradley force field model with existing infrared, Raman, and inelastic neutron scattering measurements of vibrational frequencies. Significantly, Schauble et al. [1] predict Fe isotope fractionations between Fe-cyanide compounds and metal that are similar to those predicted by Polyakov and Mineev [8]. Moreover, Schauble et al. [1] predict that speciation may play a large, if not dominant, role in determining Fe isotope fractionation; for example, they calculate a +5.6 to +5.4‰ fractionation in ^{56}Fe/^{54}Fe between $[Fe^{III}(H_2O)_6]^{3+}$ and $[Fe^{II}(H_2O)_6]^{2+}$ at 20–25°C.

We focus here on isotopic fractionation between ferric and ferrous iron in dilute aqueous solutions. Large differences in solubility between iron in its two common terrestrial oxidation states play an important role in the biological and geological processing of iron, such as transport, deposition, bioavailability, and toxicity. Ferrous solutions are geologically important, inasmuch as most Fe in hydrothermal systems exists as Fe(II) (e.g., [9–11]), and reduced Fe is likely to have been important in the Archean. However, because most Fe is in the trivalent state in the modern oceans or other near-surface environments (e.g., [12,13]), and because mobilization and precipitation processes (both biotic and abiotic) commonly involve changes in oxidation state, it is also important to assess potential isotopic fractionations involving Fe(III) species. In this contribution we demonstrate that large equilibrium isotope fractionations can occur between Fe(II) and Fe(III) in dilute aqueous solutions.

2. Analytical methods and experiment design

Determination of the kinetics of isotopic exchange and the timescales required to attain isotopic equilibrium was accomplished using enriched ^{57}Fe tracers in parallel with experiments using isotopically 'normal' iron. Our approach is somewhat similar to the 'three isotope method' [14], although distinct in that we use separate spiked and unspiked experimental runs. Some initial experiments that tested for Fe isotope fractionation during rapid precipitation with H_2O_2 were analyzed by TIMS [2]. For all other analyses, Fe isotope compositions were obtained by ICP-MS, and Fe isotope fractionation factors are in general determined more precisely using separate tracer and normal runs, relative to those obtainable using the three isotope method and conventional ICP-MS standards, as discussed in Beard et al. [15]. Distinction between kinetic and equilibrium isotope fractionation factors is important because the two may be quite different, and it has been shown for other elements that the sign and magnitude of kinetic isotope effects can be highly dependent on experimental conditions (e.g., [16–18]).

For experiments run with Fe of 'normal' iso-

topic abundances, $^{56}Fe/^{54}Fe$ and $^{57}Fe/^{54}Fe$ ratios are reported in standard δ notation [2] and were determined using multi-collector ICP-MS (Micromass *IsoProbe*), which produces external precisions of ±0.05 and ±0.07‰ (1 S.D.), respectively, on 100–300 ng total Fe. Instrumental mass bias was corrected using a 'standard-sample-standard' approach and on-peak zero background subtraction. For high-quality analyses, $^{56}Fe/^{54}Fe$–$^{57}Fe/^{54}Fe$ variations (corrected for mass bias) lie along a mass-dependent fractionation line, demonstrating complete removal of all argide interferences with the hexapole-based *IsoProbe*. For experiments run using ^{57}Fe-enriched iron, we report δ values relative to the $^{57}Fe/^{56}Fe$ ratio. Duplicate analyses were run on different days and under different plasma conditions and concentrations. See Beard et al. [15] for additional details.

Equilibrium isotope fractionation factors between Fe(III) and Fe(II) in aqueous solutions may be determined for conditions where the rate of isotopic exchange is relatively slow compared to the time required to separate the two species. In addition, because Fe(II) in aqueous solutions is always thermodynamically unstable in the presence of oxygen, the rate of oxidation must be slow relative to the timescale of separation. For example, isotopic exchange between $[Fe^{III}(H_2O)_6]^{3+}$ and $[Fe^{II}(H_2O)_6]^{2+}$ is relatively slow, due to the bond length reorganization that is required during electron transfer, but is catalyzed by chloride and, at higher pH, by hydroxide, using a group or atom transfer mechanism (e.g., [19,20]), as demonstrated using ^{55}Fe and ^{59}Fe radiotracer methods.

There are several approaches that may be taken to separate Fe(III) and Fe(II) in solution. A common method for determining Fe(II) contents is by Ferrozine® [21], and we initially investigated binding Fe(II) to Ferrozine® and Fe(III) to a siderophore (Desferol®), but enriched ^{57}Fe-tracer experiments showed that the rate at which Ferrozine® binding occurred was much slower than that of siderophore uptake. Moreover, some Fe(III) is reduced by Ferrozine®, and clean extraction of Fe from siderophores is difficult. Other workers have attempted to separate Fe(II) and Fe(III) species by chromatographic techniques, but concluded that kinetic isotope effects dominated during dissociation reactions [5]. We instead developed a method using carbonate addition to force rapid precipitation of Fe(III) by the following reaction that has been studied in flow-through reactor columns [22]:

$$Fe^{3+} + 3H_2O + 2CaCO_3\ (s) = Fe(OH)_3\ (s) + 2Ca^{2+} + HCO_3^- + H_2CO_3^0 \quad (1)$$

Here the mixed carbonate buffer system imposes a pH that is high enough to remove Fe(III), but not Fe(II). In our experiments, precipitation through carbonate addition occurred in less than 1 s. Quantitative conversion of Fe(III) to ferric precipitate under our experimental conditions (normal atmosphere) is supported by thermodynamic calculations [23,24]. Ten control runs using mixed Fe(III)–Fe(II) solutions demonstrated that conversion of Fe(III) to ferric oxyhydroxide is quantitative. In some controls, Fe(II) yields varied between 90 and 95%, and were balanced by anomalously high Fe(III) yields when Fe(III) was measured as total Fe; we interpret these results to indicate that small amounts of interstitial Fe(II) remained in the ferric oxyhydroxide precipitate during separation. Assuming a maximum of 10% Fe(II) incorporation in the ferric oxyhydroxide precipitate, the inferred $\delta^{56}Fe$ values for Fe(III) species may in some cases be too low by ~0.1‰ for experiments using 'isotopically normal' Fe and assuming Fe(III)–Fe(II) fractionation factors of 2–3‰. In contrast, the $\delta^{56}Fe$ values inferred for Fe(II) species will not be affected. The control experiments also demonstrate that no significant shift in Fe(III)/Fe(II) ratio occurred during the separation process.

No other phases were present in the precipitate based on inspection under a microscope, such as siderite, indicating that no significant Fe(II) coprecipitated with Fe(III) in our experiments. Colloidal Fe did not exist in the solutions prior to carbonate addition, based on their color and transparency. Control experiments where ferric nitrate solutions (pH ~3) were allowed to slowly precipitate produced red-orange solutions over

24 h that contained colloidal ferric iron that could not be centrifuged out; however, carbonate addition immediately flocculated the colloidal Fe, producing a transparent solution. We therefore infer that if colloidal ferric Fe is produced during our separation method, which is certainly possible, it is immediately collected with the ferric oxyhydroxide precipitate, preserving the integrity of the Fe(III) component.

Three methods of carbonate addition were used in our experiments. Initial work added ~50 mg of $CaCO_3$ directly to the Fe(III)–Fe(II) mixture, and this method was used for the enriched ^{57}Fe tracer experiments (Table 1). However, small amounts of Ca remained after ion exchange separation, producing some mass interferences from Ca species, although these were insignificant relative to the large range in isotopic compositions that were associated with the ^{57}Fe tracer experiments. Calcium interferences were nearly insignificant when reaction with $CaCO_3$ was accomplished by passing the Fe(III)–Fe(II) mixture (4 ml) through a 6×120 mm column filled with glass beads that held a thin (~1 mm) layer of $CaCO_3$ (55 mm from the top), and this method was used for data listed under Experiment 1 in Table 2. Although flow rates were relatively slow through this column (~2 ml/min), precipitation of Fe(III) occurred very rapidly at the $CaCO_3$ layer. No detectable amounts of Fe were absorbed onto the glass beads.

Although Fe(III) precipitation on the $CaCO_3$ column worked well, very low levels of CaOH interferences remained, possibly affecting the $\delta^{57}Fe/^{54}Fe$ values for Experiment 1. Our preferred method is direct addition of $BaCO_3$ (which produces no Ca-related isobars), which produces very rapid ferric oxyhydroxide precipitation and no precipitation of Fe(II), and this was used for data listed under Experiment 2 in Table 2.

The possible degree of isotopic fractionation between Fe(III) and ferric oxyhydroxide during rapid precipitation can be constrained from several experiments. Rapid oxidation of Fe(II), accompanied by rapid precipitation of ferric oxyhydroxide, produces no measurable (<0.2‰) isotopic fractionation between dissolved Fe(III) and hydrous oxide. This experiment was con-

Table 1
^{57}Fe-enriched tracer experiments

Sample		Fe(III) $\delta^{57}Fe/^{56}Fe$	$F_{[Fe(III)]}$	Fe(II) $\delta^{57}Fe/^{56}Fe$	$F_{[Fe(II)]}$	$\Delta F_{[Fe(III)-Fe(II)]}$
Initial solution		+459.6		−0.2		
5 s	[Meas.]	+243.0	0.895	+171.8	0.790	+0.105
	[Corr.]	+292.2	0.691	+137.6	0.633	+0.058
10 s	[Meas.]	+246.8	0.879	+175.4	0.807	+0.072
	[Corr.]	+278.3	0.749	+153.6	0.707	+0.042
20 s	[Meas.]	+242.9	0.895	+178.6	0.821	+0.074
	[Corr.]	+261.3	0.819	+166.0	0.764	+0.055
60 s	[Meas.]	+242.3	0.898	+210.7	0.969	−0.071
	[Corr.]	+249.3	0.869	+206.1	0.948	−0.079
180 s	[Meas.]	+222.5	0.979	+212.5	0.977	+0.002
	[Corr.]	+225.1	0.969	+211.1	0.970	−0.002

$\delta^{57}Fe/^{56}Fe$ in units of ‰. Mixtures prepared from 10 μl ^{57}Fe-enriched Fe(III) solution (1337 ppm Fe) in 4 M HCl, 13 μl of isotopically normal Fe(II) solution (831 ppm Fe, prepared from $FeCl_2$ salt), diluted with 800 μl of water, followed by brief vigorous shaking. Total Cl^- content was 49.1 mM, and pH was ~2.5 (measured by electrode) and is only approximate. Species separation accomplished by direct addition of $CaCO_3$ to mixtures at the times indicated; data for Fe(III) reflect analysis of precipitated ferric oxyhydroxide. Corrected isotope compositions obtained by subtracting effect of 20% re-equilibration during separation (see text for discussion). Fraction of isotopic exchange toward equilibrium (F; see Eq. 2) calculated based on corrected isotope compositions, and assumed equilibrium isotope composition for the average of Fe(III) and Fe(II) at 180 s ($\delta^{57}Fe/^{56}Fe = +217.5$). Although the calculated equilibrium $\delta^{57}Fe/^{56}Fe = +254.1$, based on mass balance of the initial reagents, the value inferred from the 180 s run is within the uncertainty of pipettor errors for the individual runs or the possibility that a few percent Fe(II) remained in the Fe(III) fraction (see text for discussion). Overall, the data indicate that the Fe(III):Fe(II) ratio for this experiment varied by no more than ~1.5:1 to 1:1. Difference in F calculated using Fe(III) and Fe(II) species also listed; as discussed in the text, F values are most robust based on Fe(II) measurements.

Table 2
Equilibrium fractionation experiments

Sample	$\delta^{56}Fe/^{54}Fe$ (‰)	$\delta^{57}Fe/^{54}Fe$ (‰)	μg Fe
Experiment 1: Dilute Fe-chloride solution, initial pH ~5.5, ferric precipitation by column-based $CaCO_3$ reaction			
Initial Fe(III) solution	+0.15 ± 0.07	+0.08 ± 0.03	22.78
	+0.10 ± 0.06	+0.16 ± 0.03	
Initial Fe(II) solution	−0.44 ± 0.07	−0.56 ± 0.03	25.03
Total mixture[a]	−0.14 ± 0.10	−0.24 ± 0.05	47.81
	−0.04 ± 0.08	−0.12 ± 0.04	
Final Fe(III)	+0.56 ± 0.08	+0.80 ± 0.04	47 ± 4
Final Fe(II)	−2.07 ± 0.07	−2.95 ± 0.06	8 ± 4
$\Delta_{Fe(III)-Fe(II)}$ [b]	+2.63 ± 0.11	+3.75 ± 0.07	
Experiment 2: Dilute Fe-chloride, initial pH ~2.5, ferric precipitation by bulk addition of $BaCO_3$			
Initial Fe(III) solution[c]	+0.29 ± 0.05	+0.42 ± 07	70.23
Initial Fe(II) solution	−0.44 ± 0.07	−0.56 ± 0.03	85.51
Total mixture[d]	−0.15 ± 0.06	−0.32 ± 0.04	155.74
	−0.08 ± 0.07	−0.13 ± 0.06	
Final Fe(III)	+1.25 ± 0.11	+1.91 ± 0.08	n.d.
	+1.27 ± 0.07	+1.88 ± 0.04	
Final Fe(II)	−1.51 ± 0.12	−2.31 ± 0.06	97 ± 15
	−1.46 ± 0.05	−2.21 ± 0.04	
$\Delta_{Fe(III)-Fe(II)}$ [e]	+2.75 ± 0.07	+4.16 ± 0.10	

All reagents were prepared fresh and used immediately. pH measured by electrode, and is only approximate for values <4. Errors for individual isotopic analyses based on in-run statistics (2 S.E.M.). n.d. = not determined.

[a] Mixture prepared from 12.2 mg of Fe(III) solution (6704 ppm Fe, prepared from $FeCl_3$ salt), 8.3 mg of Fe(II) solution (10 828 ppm Fe, prepared from $FeCl_2$ salt), diluted with 7.1825 g of water, followed by brief vigorous shaking. Total Cl^- content was 1.1 mM. Two ml of the mixture was passed through the $CaCO_3$ column for species separation after equilibration for 26 min. μg Fe for initial solutions (for the 2 ml of solution used) based on gravimetric determinations; μg Fe for final solutions based on Ferrozine® measurements [22].

[b] Uncertainty in isotopic fractionation based on in-run statistics. Fe(III)/Fe(II) ratio shifted from an initial value of 0.91 to 5.88 during the 26 min that the solution was allowed to stand.

[c] U.W. JM-Fe standard; measurement based on 23 analyses by ICP-MS (errors are 1σ external).

[d] Mixture prepared from 50.1 mg of Fe(III) solution (U.W. JM-Fe, 2101 ppm Fe, in 4 M HCl), 46.5 mg of Fe(II) solution (2757 ppm Fe, prepared from $FeCl_2$ salt), diluted with 9.8250 g of water, followed by brief vigorous shaking. Total Cl^- content was 21.5 mM. Species separation accomplished by adding $BaCO_3$ to 6.62 g of this mixture, after standing for 31 min.

[e] Fractionation factor calculated using averages; uncertainties calculated assuming external errors of ±0.05 and ±0.07 for $^{56}Fe/^{54}Fe$ and $^{57}Fe/^{54}Fe$, respectively (duplicates fall within this range). μg Fe for initial solutions based on gravimetric determinations; μg Fe for final Fe(II) solution based on Ferrozine® measurements. Initial Fe(III)/Fe(II) ratio was 0.82, and did not change during the 31 min standing time within the uncertainty of the final Fe(II) Fe content as determined by Ferrozine®.

ducted by rapid (<1 s) oxidation of 0.1 M ferrous sulfate (initial pH = 3.6) through addition of 30% H_2O_2, which is immediately accompanied by formation of a ferric oxyhydroxide precipitate. The pH of the remaining solution dropped to 2.9, which ceased precipitation of Fe(III) at ~50% completion. Ferrozine® analysis determined that at most 0.2% Fe(II) remained in solution, 48.0% of the Fe precipitated as ferric oxyhydroxide, and 51.8% of the Fe existed as Fe(III) in solution. $\delta^{56}Fe$ values of the precipitate and Fe(III) were identical within the 0.2‰ uncertainty of the TIMS analyses. Over much longer timescales (many hours), kinetic isotope fractionation between Fe(III) and ferric oxide during precipitation from dilute ferric nitrate solutions produces a precipitate that is 1.3‰ lighter than Fe(III) in solution [25], but the precipitation rates employed in these experiments are four to five orders of magnitude slower than that used in the Fe(III)–Fe(II) separation method discussed above. Our observations that extremely rapid precipitation produces no isotopic fractionation but moderately rapid precipitation produces signifi-

cant kinetic isotope fractionations are similar to those observed for C isotope fractionation between calcite and bicarbonate [16].

3. Results

We first focus on kinetic experiments, so that the rate law and constant for Fe isotope exchange in our experiments may be constrained. These results allow us to assess and correct for the extent of isotopic exchange during separation of Fe(III) and Fe(II) species in solution. A second set of experiments were conducted using isotopically 'normal' sources for Fe(III) and Fe(II), with the aim of determining equilibrium Fe(III)–Fe(II) isotope fractionation in solution.

3.1. Kinetics of Fe isotope exchange in solution

We have measured the kinetics of Fe isotope exchange in solution using ^{57}Fe-enriched tracers, where Fe(III) and Fe(II) species are initially $\sim$460 ‰ different (Table 1). Use of enriched tracers has the advantage that calculating the approach to equilibrium is insensitive to the value of the 'final' (equilibrium) fractionation, which is on the order of several per mil. In addition, any Fe isotope fractionation that might occur during precipitation of Fe(III) as ferric oxyhydroxide, also expected to be on the order of 1 ‰ or less (above), is insignificant when using enriched tracers. Following the approach taken by earlier workers (e.g., [26,27]), we describe the extent of exchange toward isotopic equilibrium by:

$$F = \frac{\delta - \delta_i}{\delta_e - \delta_i} \quad (2)$$

where δ_i and δ_e are the initial and equilibrium isotopic compositions, respectively, and δ is the isotopic composition at a given time. In the case of isotopic exchange between two species, it is important to note that F may be calculated using either species, and should produce the same result if the experiments are rapidly quenched relative to exchange rates. In our enriched tracer experiments, however, even small amounts of Fe(II) trapped in the ferric Fe precipitates (see above) would produce $\delta^{57}Fe/^{56}Fe$ values for the Fe(III) fraction that are too low; in this case, F values may be better constrained using the Fe(II) fraction. Substituting F into the general rate equation produces:

$$\frac{-d(1-F)}{dt} = K_n(1-F)^n \quad (3)$$

where K is the rate constant, and n is the order of the reaction, generally an integer from 0 to 3. Although most isotope exchange reactions appear to follow a first-order rate law ($n=1$) (e.g., [27]), hydrogen isotope exchange appears to follow a second-order rate law in at least some systems [26]. Integration of Eq. 3 for rate laws from $n=0$ to 3 yields the following linear forms:

$$(1-F) = -K_0 t \quad \text{for} \quad n=0 \quad (4)$$

$$\ln(1-F) = -K_1 t \quad \text{for} \quad n=1 \quad (5)$$

$$\frac{F}{(1-F)} = K_2 t \quad \text{for} \quad n=2 \quad (6)$$

$$\frac{F(F-2)}{2(F-1)^2} = K_3 t \quad \text{for} \quad n=3 \quad (7)$$

Our kinetic exchange data (Table 1) are best fit by a second-order rate law (Fig. 1), with a correlation coefficient (R^2) of 0.96 and an MSWD of 4.1; regression of the data as measured produces a rate constant $K = 0.26 \pm 0.06$ s^{-1}. The data cannot be fit to zero- or first-order laws within the constraints of Eqs. 4 and 5, respectively, in terms of linearity (both produce $R^2 < 0.2$) or intercepts (an intercept at $t=0$ of unity is required for Eq. 4 and zero for Eq. 5). The physical meaning of this empirical result is not clear. However, our present purpose is simply to correct for the effects of partial exchange during species separation on our value for $\Delta_{Fe(III)-Fe(II)}$ under our specific experimental conditions. Although the data may be reasonably fit to a third-order rate law, the MSWD increases to 9.0, and we see little justification in using such a high-order rate law. We would predict that larger rate constants would be calculated for solutions that contained higher Cl^- contents,

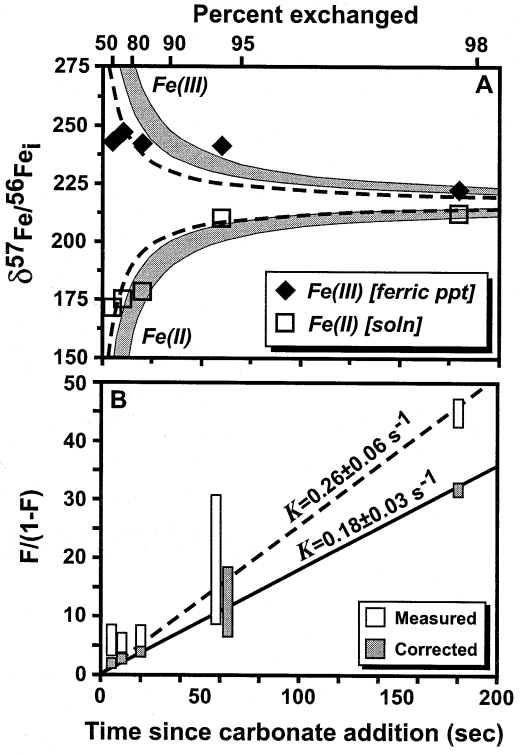

Fig. 1. Determination of the kinetics of Fe isotope exchange through use of enriched ^{57}Fe tracer experiments. Experimental runs are 'quenched' by addition of carbonate, which forces near-instantaneous (<1 s) precipitation of all Fe(III) as ferric oxyhydroxide. Initial $\delta^{57}Fe/^{56}Fe$ values were +459.6‰ and −0.2‰ for Fe(III) and Fe(II) solutions, respectively. (A) Plotted versus time, the measured data generally follow a second-order rate law where $K=0.26\pm0.06$ s^{-1} (gray band). Correction of the rate curve for 20% isotopic exchange during species separation shown by dashed line. The scatter in $\delta^{57}Fe/^{56}Fe$ values for the Fe(III) component may in part reflect small but variable amounts of interstitial Fe(II) that has low $\delta^{57}Fe/^{56}Fe$ values. The data may also have some scatter due to variations in pipetting small amounts (10–13 μl) of stock reagents (Table 1). See text for additional discussion. (B) Regression of data for second-order rate law (Eq. 6), forced through a zero intercept. Error bars reflect a 2 s error in time and range in F calculated from Fe(III) and Fe(II) species (Table 1). Data corrected for 20% isotopic exchange during species separation shown in gray bars, which results in a significantly improved fit in terms of zero intercept for data where $t\leq20$ s, error in F, and uncertainty in the calculated rate constant. The revised rate constant of $K=0.18\pm0.03$ s^{-1} is the preferred value. See text for discussion.

or in higher pH solutions, because of the importance of group or atom transfer under such conditions [19,20].

The rate constant derived from the measured ^{57}Fe tracer data indicates that ~20% isotopic exchange between Fe(III) and Fe(II) will occur in 1 s, which is the maximum estimated time in which precipitation of Fe(III) to ferric oxyhydroxide occurs. Using this rate constant, we have corrected the measured $\delta^{57}Fe/^{56}Fe$ values (Table 1) for the effects of 20% isotopic exchange during species separation, and this produces a significantly improved fit to the second-order rate equation in terms of consistency of F values calculated from both species, movement of early ($t\leq20$ s) samples toward the zero intercept, and reduced error in the calculated rate constant (Table 1, Fig. 1B). The effects of this adjustment also improves the fit of the data for the measured $\delta^{57}Fe/^{56}Fe$ values versus time (Fig. 1A). The revised rate constant of $K=0.18\pm0.03$ s^{-1} is our preferred value, and this revises the estimate for the amount of isotopic exchange during separation from 20% to 15%. Further iteration on refining the rate constant is not warranted, given the uncertainty in the timescale of the species separation process for each experimental run. In contrast, if a first-order rate law is assumed and only the longest run (180 s) is used, the percent isotopic exchange in 1 s would be <5%. It is important to note that the corrections to the data solely reflect the effects of limited isotopic exchange in solution during the separation process, and are not influenced by potential isotopic fractionation during ferric oxyhydroxide precipitation because such effects are insignificant when using enriched isotope tracers.

3.2. *Precipitation and exchange effects during species separation*

Although isotopic fractionation during precipitation of Fe(III) as ferric oxyhydroxide has no significant effect on the ^{57}Fe-enriched tracer experiments, such fractionation may potentially affect exchange experiments using 'normal' isotopic compositions. Isotopic fractionation during precipitation can be modeled using an increment method and simple mass-balance constraints:

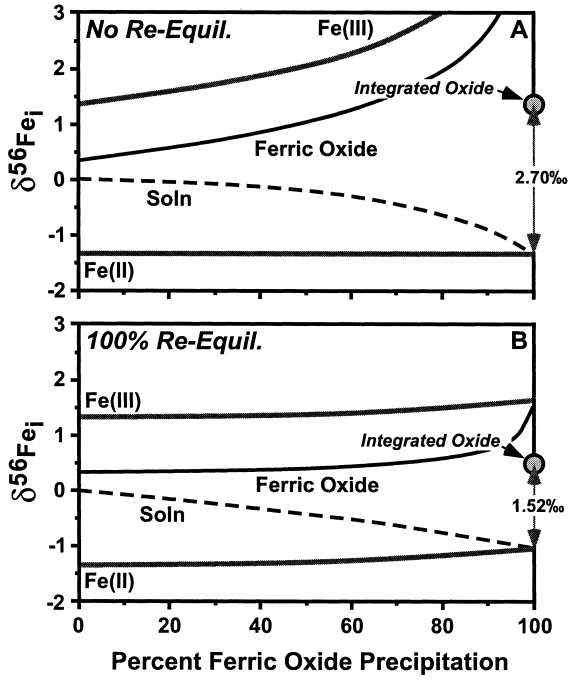

Fig. 2. Calculated effects on measured fractionation between ferric oxyhydroxide precipitate and remaining Fe(II) in solution assuming a +1.0‰ fractionation between Fe(III) and ferric oxyhydroxide during species separation. The equilibrium Fe(III)–Fe(II) fractionation is assumed to be +2.7‰. Fractionation during precipitation is assumed to follow a Rayleigh distillation process. Curves shown for the instantaneous isotopic compositions of Fe(III), ferric oxide precipitate, Fe(II), and total solution [Fe(III) and Fe(II)]; integrated oxide composition also shown after 100% precipitation. Model constructed using incremental calculations and Eqs. 8–11. (A) In the case where no Fe(III)–Fe(II) re-equilibration occurs, the δ^{56}Fe value of Fe(II) is constant, and $\Delta_{\mathrm{Fe(III)-ferric\ oxide}}$ is fixed. Because the Fe(III)→ferric oxide reaction goes to completion, and there is no re-equilibration between Fe(III) and Fe(II), the δ^{56}Fe value of the total precipitate will accurately reflect the δ^{56}Fe value of initial Fe(III) in solution, allowing the equilibrium $\Delta_{\mathrm{Fe(III)-Fe(II)}}$ to be directly determined from isotopic measurements of the precipitate and remaining Fe(II) in solution. (B) In the case where complete (100%) isotopic equilibration between Fe(III) and Fe(II) is maintained during precipitation, and when there is a significant (+1.0‰) fractionation between Fe(III) and ferric oxyhydroxide, $\Delta_{\mathrm{Fe(III)-Fe(II)}}$ remains constant, and the δ^{56}Fe values of the precipitate and Fe(II) are controlled by the mass balance of the system over time. The integrated δ^{56}Fe value of the ferric oxide and the δ^{56}Fe value of the final Fe(II) in solution underestimate the initial $\Delta_{\mathrm{Fe(III)-Fe(II)}}$ of the solution by 1.2‰ in this extreme case.

$$\delta_{\mathrm{MIX}} = X^{\mathrm{M}}_{\mathrm{Fe(III)}}\delta_{\mathrm{Fe(III)}} + X^{\mathrm{M}}_{\mathrm{Fe(II)}}\delta_{\mathrm{Fe(II)}} \quad (8)$$

in addition to the isotopic fractionation factors, defined as:

$$\Delta_{\mathrm{Fe(III)-Fe(II)}} = \delta_{\mathrm{Fe(III)}} - \delta_{\mathrm{Fe(II)}} \approx 10^3 \ln \alpha_{\mathrm{Fe(III)-Fe(II)}} \quad (9)$$

and

$$\Delta_{\mathrm{Fe(III)-ferric\ oxide}} = \delta_{\mathrm{Fe(III)}} - \delta_{\mathrm{ferric\ oxide}} \approx 10^3 \ln \alpha_{\mathrm{Fe(III)-ferric\ oxide}} \quad (10)$$

We also assume that isotopic fractionation during precipitation occurs by Rayleigh distillation, which is described by:

$$\delta_{\mathrm{A}} = F^{[\alpha_{A-B}-1]}\,(1000 + \delta^{i}_{\mathrm{A}}) - 1000 \quad (11)$$

In the case where there is no isotopic re-equilibration between Fe(III) and Fe(II) during precipitation of ferric oxyhydroxide even if $\Delta_{\mathrm{Fe(III)-ferric\ oxide}}$ is not zero, there will be no error introduced in the measured $\Delta_{\mathrm{Fe(III)-Fe(II)}}$ if precipitation of Fe(III) goes to completion. For this case, $\Delta_{\mathrm{Fe(III)-ferric\ oxide}}$ is fixed, producing a range in $\Delta_{\mathrm{Fe(III)-Fe(II)}}$ during precipitation (Fig. 2A). Although the δ^{56}Fe values for Fe(III), ferric oxide, and the total solution change during precipitation (Fig. 2A), the total precipitate will be equal in composition to the original Fe(III) in solution, allowing the correct $\Delta_{\mathrm{Fe(III)-Fe(II)}}$ to be determined. In contrast, for the case where 100% re-equilibration between Fe(III) and Fe(II) occurs during precipitation, significant errors will be introduced when attempting to determine the equilibrium $\Delta_{\mathrm{Fe(III)-Fe(II)}}$. For these conditions, $\Delta_{\mathrm{Fe(III)-Fe(II)}}$ is fixed, and the apparent $\Delta_{\mathrm{Fe(III)-ferric\ oxide}}$ varies as the proportion of Fe(III) decreases. The integrated δ^{56}Fe value of the ferric oxide will be significantly underestimated, and the final δ^{56}Fe value of Fe(II) will be shifted to higher values when equilibrium between Fe(III) and Fe(II) is maintained, resulting in a significant underestimation of the initial (true) $\Delta_{\mathrm{Fe(III)-Fe(II)}}$ value (Fig. 2B).

Combining the effects of partial to complete re-

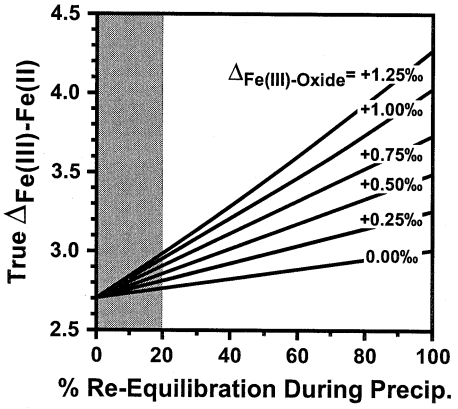

Fig. 3. Summary of the effects of 0–100% re-equilibration between Fe(III) and Fe(II) during species separation and 0 to +1.25‰ fractionation between Fe(III) and ferric oxyhydroxide during precipitation, following the model illustrated in Fig. 2. Based on the initial rate constant ($K = 0.26$ s^{-1}), a maximum of 20% isotopic exchange is estimated to occur during Fe(III)–Fe(II) species separation (gray band). Using the revised rate constant of $K = 0.18$ s^{-1} indicates that ~15% isotopic exchange occurred during species separation. In either case, very small errors are introduced for the inferred equilibrium $\Delta_{Fe(III)-Fe(II)}$ value for our experiments.

equilibration between Fe(III) and Fe(II) and isotopic fractionation during precipitation of ferric oxyhydroxide indicates that the greatest errors in determination of the true $\Delta_{Fe(III)-Fe(II)}$ occur when $\Delta_{Fe(III)-ferric\ oxide}$ is large and the extent of Fe(III)–Fe(II) re-equilibration is also large (Fig. 3). Based on the 15–20% re-equilibration during separation that is estimated from the kinetic experiments, an error of less than 0.1‰ is introduced in determination of the true $\Delta_{Fe(III)-Fe(II)}$ if no significant isotopic fractionation occurs during precipitation. If precipitation were associated with a very large $\Delta_{Fe(III)-ferric\ oxide}$, such as +1.0‰, the measured $\Delta_{Fe(III)-Fe(II)}$ would be ~0.3‰ too low at ~20% re-equilibration during separation (Fig. 3); however, as noted above, we see no evidence that such high $\Delta_{Fe(III)-ferric\ oxide}$ exists during very rapid precipitation of Fe(III).

3.3. Equilibrium Fe isotope fractionation in solution

Experiments that used isotopically 'normal' solutions measure an apparent $\Delta_{Fe(III)-Fe(II)} = +2.7$‰ for $^{56}Fe/^{54}Fe$ in dilute aqueous solutions at room temperature (22 ± 2°C). In one experiment (Experiment 1, Table 2), a dilute Fe(III)–Fe(II) solution (1.1 mM Cl^-) at pH = 5.5 was allowed to stand for 26 min. However, at this pH, OH^- contents are sufficiently high to allow significant oxidation over the timescale of the experiment (e.g., [19,20]), and this is reflected in a shift in Fe(III)/Fe(II) ratio from 0.91 to 5.88 over the 26 min experiment (Table 2). The shift in Fe(III)/Fe(II) ratio measured for the final solutions is consistent with the shift in mass balance of the Fe isotope compositions of the separated species (Table 2). No precipitation of Fe(III) occurred over the time of the experiment. The rate constant measured for Fe(III)–Fe(II) exchange suggests that isotopic equilibration could be maintained in this experiment despite the large shift in Fe(III)/Fe(II) ratio.

A second experiment involved a Fe(III)–Fe(II) solution with higher ionic strength (21.5 mM Cl^-) that was moderately acidic (pH ~2.5) (Experiment 2, Table 2), which prevents oxidation of Fe(II) on the timescales of the experiment (31 min). The initial Fe(III)/Fe(II) ratio was 0.82 (determined by gravimetry), and the Fe(II) content of the separated species is unchanged, within the uncertainty limit of the Ferrozine measurements (Table 2). This is independently confirmed by the mass balance constraints of the Fe isotope compositions of the separated species (Table 2). That the $\Delta_{Fe(III)-Fe(II)}$ value measured for both experiments is the same within analytical error is consistent with the rate constants determined for Fe(III)–Fe(II) exchange and the timescales of the experiments. Based on modeling the isotopic effects during our separation process, we estimate that the true $\Delta_{Fe(III)-Fe(II)} = +2.75 \pm 0.15$‰ for our experimental conditions.

4. Discussion

There is widespread agreement from Raman, UV, and IR spectroscopic work, as well as X-ray diffraction and EXAFS studies, that in dilute ferrous chloride solutions near room temperature, Fe(II) is octahedrally coordinated by water as $[Fe^{II}(H_2O)_6]^{2+}$ (e.g., [28–31]). Fe–O bond lengths

involving water in the first hydration sphere are, however, affected by total Cl^- contents and Fe/Cl ratios, where bond lengths are increased by increasing Fe/Cl ratios or total Cl^- [29]; these effects might produce differences in reduced partition function ratios of ferrous hexaquo complexes, where, all else being equal, the longer Fe–O bonds would favor the light isotope. The speciation of ferric solutions is more complicated, representing a spectrum between octahedrally coordinated water and chloride species and tetrahedrally coordinated chloride species (e.g., [32]). For example, XRD, Raman, and EXAFS studies show that at low [Fe] and moderate [Cl^-] (<8 M), Fe(III) speciation is largely $[Fe^{III}(H_2O)_6]^{3+}$, whereas in solutions prepared by dissolution in HCl, or those that have high [Cl^-] (>11 M), the major species is $[Fe^{III}Cl_4]^-$, particularly if the high Cl^- contents are achieved using LiCl (e.g., [29,32–36]). However, significant amounts of mixed coordination of water and chloride have been identified in many studies that have moderate [Fe] and [Cl^-], and involve a range of Fe:Cl stoichiometries, from $[Fe^{III}Cl_2(H_2O)_4]^+$ to $[Fe^{III}Cl_5H_2O]^{2-}$ [29,34,35]. Inada and Funahashi [37] used EXAFS measurements to identify the monochloro complex $[Fe^{III}(H_2O)_5Cl]^{2+}$, and, importantly, report that incorporation of chloride leads to lengthening of the Fe–O bond. Both this bond lengthening and the replacement of water by chloride should decrease the affinity of Fe(III) complexes for the heavy isotopes of Fe; this behavior is predicted from vibrational spectra, and by the calculations of Schauble et al. [1].

Thermodynamic calculations suggest that in our experiments $>97\%$ Fe(II) exists as $[Fe^{II}(H_2O)_6]^{2+}$, and $>82\%$ Fe(III) exists as $[Fe^{III}(H_2O)_6]^{3+}$ and $[Fe^{III}(H_2O)_{6-n}(OH)_n]^{3-n}$ (Table 3). Because Fe–O bonding is the primary control on Fe isotope fractionation, we do not anticipate significant differences in the reduced partition function ratio for $[Fe^{III}(H_2O)_6]^{3+}$ or $[Fe^{III}(H_2O)_{6-n}(OH)_n]^{3-n}$; that the fractionations measured for Experiments 1 and 2 agree, despite large differences in the calculated abundances of $Fe^{III}(OH)_n$ species, lends some support to this idea, in contrast to the inferences of Bullen et al. [6]. Significant Fe chloride species are calculated for Experiment 2, ranging from 3 to 18% depending upon the database used for calculation. That the $\Delta_{Fe(III)-Fe(II)}$ measured for Experiments 1 and 2 are the same within analytical error and the uncertainties produced by species separation indicates that if differences exist in hydroxide and chloride speciation between the two experiments, this is not accompanied by significant differences in isotopic fractionation.

The +2.7‰ equilibrium fractionation in $^{56}Fe/^{54}Fe$ we measure for aqueous Fe(III)–Fe(II) equilibria is qualitatively similar to those predicted by

Table 3
Calculated percent species for ^{57}Fe tracer and isotopically 'normal' experiments

	Ferric Fe						Ferrous Fe	
	$[Fe]^{3+}$	$[Fe(OH)]^{2+}$	$[Fe(OH)_2]^+$	$[Fe(OH)_3]^0$	$[FeCl]^{2+}$	$[FeCl_2]^+$	$[Fe]^{2+}$	$[FeCl]^+$
^{57}Fe tracer experiment (Table 1):								
GWB	0.1	11.7	87.2	0.9	0.0	0.0	99.8	0.2
PHREEQC	0.1	11.8	87.8	0.3	0.0	0.0	99.9	0.1
MINEQL+	0.0	0.0	98.5	1.2	0.0	0.0	97.0	3.0
'Normal' isotope composition, Experiment 1 (Table 2):								
GWB	0.0	0.9	87.2	11.9	0.0	0.0	99.9	0.1
PHREEQC	0.0	1.0	95.2	3.7	0.0	0.0	99.9	0.1
MINEQL+	0.0	0.9	98.7	0.0	0.0	0.0	99.9	0.1
'Normal' Isotope Composition, Experiment 2 (Table 2):								
GWB	36.7	55.3	4.7	0.0	3.1	0.0	99.3	0.7
PHREEQC	35.6	46.8	3.5	0.0	13.2	0.8	98.1	1.9
MINEQL+	25.2	51.4	5.4	0.0	16.3	1.6	98.7	1.3

Other species $<0.4\%$. H_2O not listed in species for clarity. References: GWB (Geochemist's Workbench [23]), using LLNL database [24]. PHREEQC [38], using WATEQ4F database [39]. MINEQL+ [40], using NIST Database 46 (version 6) [41].

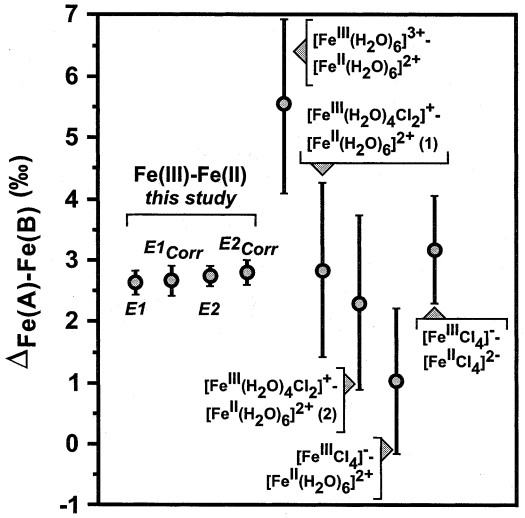

Fig. 4. Comparison of measured Fe isotope fractionation [$\Delta_{Fe(A)-Fe(B)}$] between various Fe(III) and Fe(II) species in aqueous solutions at 22°C. Error bars shown for all fractionations. Results for U.W. Madison Experiments shown on left (this study). *E1* = measured data for Experiment 1 (Table 2); $E1_{Corr}$ = data corrected for 0.1‰ shift during precipitation (see text); *E2* = measured data for Experiment 2 (Table 2); $E2_{Corr}$ = data corrected for 0.1‰ shift during precipitation. Also shown are predicted fractionations from Schauble et al. [1]; errors from Schauble et al. Predicted fractionations involving $[Fe^{III}(H_2O)_4Cl_2]^+$ shown for two methods of calculation ['(1)' and '(2)'] of the reduced partition function ratio for this species [1]. Based on thermodynamic calculations (Table 3), we infer that >97% Fe(II) exists as $[Fe^{II}(H_2O)_6]^{2+}$, and >82% Fe(III) exists as $[Fe^{III}(H_2O)_6]^{3+}$ and $[Fe^{III}(H_2O)_{6-n}(OH)_n]^{3-n}$, and this is supported by spectroscopic studies. We do not anticipate significant differences in the reduced partition function ratios for $[Fe^{III}(H_2O)_6]^{3+}$ and $[Fe^{III}(H_2O)_{6-n}(OH)_n]^{3-n}$. Assuming that as much as 18% of Fe(III) exists as ferric chloride complexes in our Experiment 2 (Table 3), the calculations of Schauble et al. [1] predict a shift in $\Delta_{Fe(III)-Fe(II)}$ of ~0.25‰; this difference is not seen between Experiment 1 and Experiment 2.

Schauble et al. [1]. If the dominant ferric and ferrous species in our very dilute solutions are indeed $[Fe^{III}(H_2O)_6]^{3+}$ or $[Fe^{III}(H_2O)_{6-n}(OH)_n]^{3-n}$ and $[Fe^{II}(H_2O)_6]^{2+}$, respectively, then our results indicate that the $^{56}Fe/^{54}Fe$ fractionation is approximately a factor of two less that that predicted by Schauble et al. [1] at 25°C. Schauble et al. [1] predict significant changes in reduced partition function ratios for Fe(III) with addition of Cl^- (Fig. 4); if ferric chloride species comprise up to 18% of Fe(III) in Experiment 2 (Table 3), then $\Delta_{Fe(III)-Fe(II)}$ is predicted to be 0.25‰ less than that of a system that had no ferric chloride species. Schauble et al. [1] estimate that the uncertainty in the reduced partition function ratios for $[Fe^{III}(H_2O)_6]^{3+}$ and $[Fe^{II}(H_2O)_6]^{2+}$ at 25°C is ≥0.9‰, although this does not include possible errors in the IR data used in their calculations. Combined, these estimates suggest an uncertainty of ~±1.4‰ for the predicted $\Delta_{Fe(III)-Fe(II)}$ at 25°C. Although additional uncertainties exist regarding the effects of Cl^- and exact speciation in our experiments, approximately 1‰ remains unaccounted for when comparing our experimental results with theory.

The most remarkable result of our experiments is that the isotopic fractionation between Fe(III) and Fe(II) in solution spans virtually the entire range observed in terrestrial sedimentary rocks [2,3,7], indicating that aqueous speciation may play a major role in determining Fe isotope variations in nature where different iron species can become separated; even if both types of Fe eventually assume the same chemical form, these differences may persist. Although previous experimental work has suggested a major role for speciation in determining Fe isotope fractionation [4–6], none of these studies demonstrated attainment of isotopic equilibrium. Furthermore, these experiments involved interpretation of demonstrably kinetic effects, unknown influences by precipitation, or inferred that steady-state, flow-through reactors approach equilibrium conditions.

We conclude by reviewing our results in light of our previous biological experiments where Fe-reducing bacteria were found to produce a +1.3‰ fractionation in $^{56}Fe/^{54}Fe$ between ferric substrate and Fe(II) [3]. We have interpreted this fractionation to reflect an overall kinetic isotope or 'vital' effect, similar to what has been measured, for example, for C isotopes (e.g., [42,43]). Although the exact process by which *Shewanella alga* reduces Fe is not clear, several steps are possible, including dissolution of the ferric substrate, transport of dissolved Fe(III) to the cell (or direct attachment of the cell to Fe^{3+} on the substrate surface), binding of Fe(III) at the site of reduction, and Fe reduction and release of Fe(II) (e.g., [44–48]). We would not expect significant isotopic fraction-

ation during simple dissolution of ferric substrate at low temperatures, assuming dissolution occurs smoothly along an advancing dissolution front in an isotopically homogeneous crystal, at rates that are much faster than solid-state diffusion. However, our results suggest that if Fe(III) is transported to the cell, the exact nature of the ligand may have a strong effect on the isotopic fractionation of the process. Understanding the relative contributions of biologic and equilibrium isotopic fractionations to production of iron isotope anomalies in nature will require a detailed understanding of the specific pathways in which biological processing of iron occurs.

Acknowledgements

This research was supported by NSF Grants EAR-9905436 and EAR-9903252, the NASA Astrobiology Institute and Exobiology Program, and the Welch Foundation (Grant B-1445). We thank Edwin Schauble for sharing his results with us prior to publication, Greg Druschel and Martin Shafer for making the thermodynamic calculations, and Sue Welch for sharing the results of her control experiments. Three anonymous reviewers provided comments that greatly helped to sharpen the discussion. *[EB]*

References

[1] E.A. Schauble, G.R. Rossman, H.P. Taylor Jr., Theoretical estimates of equilibrium Fe-isotope fractionations from vibrational spectroscopy, Geochim. Cosmochim. Acta 65 (2001) 2487–2497.

[2] B.L. Beard, C.M. Johnson, High precision iron isotope measurements of terrestrial and lunar materials, Geochim. Cosmochim. Acta 63 (1999) 1653–1660.

[3] B.L. Beard, C.M. Johnson, L. Cox, H. Sun, K.H. Nealson, C. Aguilar, Iron isotope biosignatures, Science 285 (1999) 1889–1892.

[4] A.D. Anbar, J.E. Roe, J. Barling, K.H. Nealson, Nonbiological fractionation of iron isotopes, Science 288 (2000) 126–128.

[5] A. Matthews, X.-K. Zhu, K. O'Nions, Kinetic iron stable isotope fractionation between iron (-II) and (-III) complexes in solution, Earth Planet. Sci. Lett. 192 (2001) 81–92.

[6] T.D. Bullen, A.F. White, C.W. Childs, D.V. Vivit, M.S. Schulz, Demonstration of significant abiotic iron isotope fractionation in nature, Geology 29 (2001) 699–702.

[7] X.-K. Zhu, R.K. O'Nions, Y. Guo, B.C. Reynolds, Secular variation of iron isotopes in North Atlantic Deep Water, Science 287 (2000) 2000–2002.

[8] V.B. Polyakov, S.D. Mineev, The use of Mössbauer spectroscopy in stable isotope geochemistry, Geochim. Cosmochim. Acta 64 (2000) 849–865.

[9] D.A. Crerar, N.J. Susak, M. Borcsik, S. Schwartz, Solubility of the buffer assemblage pyrite+pyrrhotite+magnetite in NaCl solutions from 200 to 350°C, Geochim. Cosmochim. Acta 42 (1978) 1427–1437.

[10] S.A. Wood, D.A. Crerar, M.P. Borcsik, Solubility of the assemblage pyrite-pyrrhotite-magnetite-sphalerite-galena-gold-stibnite-bismuthinite-argentite-molybdenite in H_2O-NaCl-CO_2 solutions from 200 to 350°C, Econ. Geol. 82 (1987) 1864–1887.

[11] K. Ding, W.E. Seyfried Jr., Determination of Fe-Cl complexing in the low pressure supercritical region (NaCl fluid): Iron solubility constraints on pH of subseafloor hydrothermal fluids, Geochim. Cosmochim. Acta 56 (1992) 3681–3692.

[12] F.J. Millero, W. Yao, J. Aicher, The speciation of Fe(II) and Fe(III) in natural waters, Mar. Chem. 50 (1995) 21–39.

[13] E.L. Rue, K.W. Bruland, Complexation of iron(III) by natural organic ligands in the Central North Pacific as determined by a new competitive ligand equilibration/adsorptive cathodic stripping voltammetric method, Mar. Chem. 50 (1995) 117–138.

[14] Y. Matsuhisa, J.R. Goldsmith, R.N. Clayton, Mechanism of hyrothermal recrystallization of quartz at 250°C and 15 kb, Geochim. Cosmochim. Acta. 42 (1978) 173–183.

[15] B.L. Beard, C.M. Johnson, J.L. Skulan, K.H. Nealson, L. Cox, H. Sun, Application of Fe isotopes to tracing the geochemical and biological cycling of Fe, Chem. Geol. (2002) in press.

[16] J.V. Turner, Kinetic fractionation of carbon-13 during calcium carbonate precipitation, Geochim. Cosmochim. Acta 46 (1982) 1183–1191.

[17] C.S. Romanek, E.L. Grossman, J.W. Morse, Carbon isotopic fractionation in synthetic aragonite and calcite: effects of temperature and precipitation rate, Geochim. Cosmochim. Acta 56 (1992) 419–430.

[18] S.-T. Kim, J.R. O'Neil, Equilibrium and nonequilibrium oxygen isotope effects in synthetic carbonates, Geochim. Cosmochim. Acta 61 (1997) 3461–3475.

[19] J. Silverman, R.W. Dodson, The exchange reaction between the two oxidation states of iron in acidic solutions, J. Phys. Chem. 56 (1952) 846–852.

[20] R.J. Campion, T.J. Conocchioli, N. Sutin, The inner-sphere activated complex for the electron exchange of iron(II) and the monochloro complex of iron(III), Inorg. Chem. 5 (1964) 4591–4594.

[21] M. Dawson, S. Lyle, Spectrophotometric determination of iron and cobalt with *Ferrozine* and dithiozone, Talanta 37 (1990) 1189–1192.

[22] A.E. Fryar, F.W. Schwartz, Hydraulic-conductivity reduction, reaction-front propagation, and preferential flow within a model reactive barrier, J. Contamin. Hydrol. 32 (1998) 333–351.
[23] C.M. Bethke, Geochemist's Workbench 3.1: A User's Guide to Rxn, Act2, Tact, React, and Gtplot, University of Illinois, Urbana, IL, 2000, 214 pp.
[24] J.M. Delany, S.R. Lundeen, The LLNL thermochemical database, Lawrence Livermore National Laboratory Rep. UCRL-21658, 1990, 150 pp.
[25] J.L. Skulan, H. Sun, B. Beard, J. O'Leary, C. Johnson, K. Nealson, Progress in the development of an iron isotope biosignature, EOS Suppl. (2000) S30.
[26] C.M. Graham, Experimental hydrogen isotope studies III: Diffusion of hydrogen in hydrous minerals, and stable isotope exchange in metamorphic rocks, Contrib. Mineral. Petrol. 76 (1981) 216–228.
[27] R.E. Criss, R.T. Gregory, H.P. Taylor Jr., Kinetic theory of oxygen isotope exchange between minerals and water, Geochim. Cosmochim. Acta 51 (1987) 1099–1108.
[28] H. Kanno, J. Hiraishi, A Raman study of aqueous solutions of ferric nitrate, ferrous chloride and ferric chloride in the glassy state, J. Raman Spectrosc. 12 (1982) 224–227.
[29] M.J. Apted, G.A. Waychunas, G.E. Brown, Structure and specification of iron complexes in aqueous solutions determined by X-ray absorption spectroscopy, Geochim. Cosmochim. Acta 49 (1985) 2081–2089.
[30] L.V. Koplitz, D.S. McClure, D.A. Crerar, Spectroscopic study of chloroiron(II) complexes in LiCl-DC1-D_2O solutions, Inorg. Chem. 26 (1987) 308–313.
[31] C.A. Heinrich, T.M. Seward, A spectrophotometric study of aqueous chloride complexing from 25°C to 200°C, Geochim. Cosmochim. Acta 54 (1990) 2207–2221.
[32] C.L. Standley, R.F. Kruh, On the structure of ferric chloride solutions, J. Chem. Phys. 34 (1961) 1450–1451.
[33] G.W. Brady, M.B. Robin, J. Varimbi, The structure of ferric chloride in neutral and acid solutions, Inorg. Chem. 3 (1964) 1168–1173.
[34] S.K. Sharma, Raman study of ferric chloride solutions and hydrated metals, J. Chem. Phys. 60 (1974) 1368–1375.
[35] S.K. Sharma, V.N. Sehgal, H.L. Bami, S.D. Sharma, Raman study of the structure of ferric chloride in frozen aqueous solutions, J. Inorg. Nucl. Chem. 37 (1975) 2417–2419.
[36] M. Magini, T. Radnai, X-ray diffraction study of ferric chloride solutions and hydrated melt. Analysis of the iron (III)-chloride complexes formation, J. Chem. Phys. 71 (1979) 4255–4262.
[37] Y. Inada, S. Funahashi, Equilibrium and structural study of chloro complexes of iron(III) in acidic aqueous solution by means of x-ray absorption spectroscopy, Z. Naturforsch. B Chem. Sci. 54 (1999) 1517–1523.
[38] D.L. Parkhurst, C.A.J. Appelo, User's guide to PHREEQC (ver. 2) – A computer program for speciation, batch-reaction, one-dimensional transport, and inverse geochemical calculations, US Geol. Surv. Water Res. Invest. Rep. 99-4259 (1999) 312 pp.
[39] J.W. Ball, D.K. Nordstrom, WATEQ4F – User's manual with revised thermodynamic database and test cases for calculating speciation of major, trace, and redox elements in natural waters, US Geol. Surv. Open-File Rep. 90-129 (1991) 185 pp.
[40] W.D. Schecher, D.C. McAviy, MINEQL+: A chemical equilibrium program for personal computers, Environ. Res. Software, Hallowell, ME, 1994.
[41] R.M. Smith, A.E. Martell, Critically selected stability constants of metal complexes, NIST Std. Ref. Database 46, ver. 6.0, Natl. Inst. Stds. Tech., Gaithersburg, MD, 2001.
[42] G. Wefer, W.H. Berger, Isotope paleontology: growth and composition of extant calcareous species, Mar. Geol. 100 (1991) 207–248.
[43] A.C. Ravelo, R.G. Fairbanks, Carbon isotopic fractionation in multiple species of planktonic foraminifera from core-tops in the tropical Atlantic, J. Foraminifer. Res. 25 (1995) 53–74.
[44] S. Gespard, F. Vazques, C. Holliger, Localization and solubilization of the Fe(II) reductase of *Geobacter sulfurreducens*, Appl. Environ. Microbiol. 64 (1998) 3188–3194.
[45] J.H. Forsythe, P.A. Maurice, L.E. Hersman, Attachment of *Pseudomonas* sp. to Fe(III)-(hydr)oxide surfaces, Geomicrobiol. J. 15 (1998) 293–308.
[46] K.P. Nevin, D.R. Lovley, Lack of production of electron-shuttling compounds or solubilization of Fe(III) during reduction of insoluble Fe(III) oxide by *Geobacter metallireducens*, Appl. Environ. Microbiol. 66 (2000) 2248–2251.
[47] D.K. Newmann, R. Kolter, A role for excreted quinones in extracellular electron transfer, Nature 405 (2000) 94–97.
[48] H.C. Doug, J.K. Frederickson, D.W. Kennedy, J.M. Zachara, D.W. Kukkadapu, T. Onstott, Mineral transformation associated with microbial reduction of magnetite, Chem. Geol. 169 (2000) 299–318.